2014 IEEE International Conference on Robotics & Automation (ICRA)
Hong Kong Convention and Exhibition Center
May 31 - June 7, 2014. Hong Kong, China

Visibility-oriented Coverage Control of Mobile Robotic Networks on Non-convex Regions

Yiannis Kantaros[1], Michalis Thanou[2] and Anthony Tzes[2]

***Abstract*— In this paper, the area coverage problem of non-convex environments by a group of mobile robots is addressed. Each robot is equipped with a sensing device modeled through a range-limited visibility field. The network is assumed to be homogeneous in terms of nodes' sensing capabilities and general characteristics. A gradient-ascent control law is proposed, based on visibility-based Voronoi diagrams, leading the network to the optimal final state in terms of total area coverage. The provided simulation studies illustrate the results derived by the application of the proposed control scheme and validate its effectiveness.**

***Index Terms*— Non-convex area coverage problem,visibility-based Voronoi diagrams,mobile robotic networks**

I. Introduction

Extensive research has been conducted in the field of multi-robot systems in the last decades. The scientific motivation for studying different aspects of robotic networks stems from the observation of the swarming behavior of animals, that can perform complex tasks when they are working in groups. In a similar way, a group of mobile robots with sensing, communication and computational capabilities can be successfully used for a wide range of applications such as search and rescue missions [1], environmental coverage [2] and area mapping [3].

An application of mobile robotic networks that has attracted the research attention is the area coverage problem, where a given domain of interest has to be sensed by a group of mobile nodes. Several distributed coordination schemes have been proposed by researchers in the specific field. The majority of them assume convex domains of interest. In [4] the authors proposed a distributed control law based on Lloyd's algorithm and the Voronoi diagrams, for leading a mobile sensor homogeneous network in a local optimal state that maximizes the total sensing performance of the network. In [5] a different scheme was presented in case of range-limited, uniform sensing patterns that locally maximizes the total area covered by the network. Many research activities extended these works for networks with either heterogeneous [6–8] or anisotropic [9–11] sensing capabilities. Another extension of [4] is presented in [12, 13] where RF communication constraints are imposed on the sensor network.

Nevertheless, these coordination schemes are inapplicable in non-convex areas since signal attenuation caused by non-convexities of the environment is ignored. Therefore, several coordination techniques have been proposed for coverage of concave areas. The authors in [14, 15] present a technique for transforming a class of non-convex regions into convex ones using a diffeomorphism. Having achieved that, the control law presented in [4] can be applied in the transformed convex region and via the reverse process the real nodes' trajectories in the non-convex area can be obtained. The use of the geodesic distance instead of the standard Euclidean one has been proposed in [16] where the authors proposed a control scheme that drives the nodes to a generalized centroid of their Voronoi cells minimizing a coverage-based cost function. The authors in [17] studied the case where the area of interest is not known a-priori. They used an entropy (or uncertainty) metric as density function in order to allow the nodes to cover and explore the environment at the same time.

Another coordination strategy is proposed in [18], based on Lloyd's algorithm and on Euclidean Voronoi tessellation, that leads the nodes to the projected centroid of a virtual Voronoi cell. However, this results in a sub-optimal final state since in this way the coverage of the convex hull of the area is maximized. In [19] the authors propose a solution based on potential fields, where each node receives repulsive forces from other robots and obstacles, while in [20] an attractive force to the centroid of the corresponding Voronoi cell is added. A distributed control scheme based on geodesic-disc sensor footprint is presented in [21, 22] where the nodes converge to a local optimum of an area function. Also, a visibility-based algorithm is presented in [23] while in [24] a visibility coverage-oriented approach is proposed for solving an art gallery problem.

The main contribution of this paper is a coordination scheme for area coverage of non-convex environments, assuming a mobile robotic network with visibility-based sensors. The optimality of the algorithm and the monotonicity of the coverage performance through network evolution are guaranteed. The rest of this article is organized as follows: In section II the coverage problem is described along with assumptions concerning the capabilities of each mobile robot. In section III the proposed coordination scheme is presented while in IV its efficiency is verified via numerical simulations. Concluding remarks are presented in the last section.

II. Visibility-Coverage Problem Formulation for Concave Regions

Consider a group of n mobile robots (also referred to as "nodes") responsible for the coverage of a concave area

[1] Yiannis Kantaros is with the Dept. of Mechanical Engineering & Materials Science, Duke University, Durham, NC, USA

[2] Michalis Thanou and Anthony Tzes are with the Electrical & Computer Engineering Department, University of Patras, Rio, Achaia 26500, Greece

Corresponding author's e-mail: yiannis.kantaros@duke.edu

denoted as $A \subset \mathbb{R}^2$. The density function $\phi(q) : A \subset \mathbb{R}^2 \to \mathbb{R}_+$ determines the importance of any point $q \in A$ from coverage perspective. The set $X = \{x_1, x_2, ..., x_n\} \subset A$ represents the nodes' positions in the domain of interest while their motion is described by the following first order differential equation:

$$\frac{\mathrm{d}}{\mathrm{d}t}(x_i) = u_i, \quad u_i \in \mathbb{R}^2, \; x_i \in A, \; i = 1, \ldots, n, \tag{1}$$

where u_i is the control input.

Assuming area coverage purposes, each node is equipped with a device with sensing capabilities. In this article, the mobile robotic platforms are assumed to be equipped with omnidirectional camera-sensors. Before providing a formal definition of such a pattern, it is essential to define the visibility polygon of an arbitrary node.

Definition 1: The visibility polygon of an arbitrary node i, denoted as VP_i, is defined as the set of points $q \in A$ that are visible from i, that is

$$VP_i = \{q \in A | [x_i, q] \in A\} \ , \tag{2}$$

where $[x_i, q]$ is the closed segment connecting x_i and q.

Considering the definition of the visibility polygon along with the fact that a camera may have a range-limited field of view, one can define the visibility disc (right part of Fig. 1) as follows.

Definition 2: The visibility disc of a node i, denoted as C_i, is defined as the set of points $q \in VP_i$ being in distance less or equal to r, that is

$$C_i = \{q \in VP_i \cap B_i\} \ , \tag{3}$$

where $B_i = \{q \in A | \, \|q - x_i\| \leq r\}$.

Assumption 1: Each node is assumed to be equipped with an omnidirectional camera-sensor sensing all the points of the domain of interest lying in its visibility disc as defined in (3) while sensing range, r is assumed to be fixed and common for all nodes.

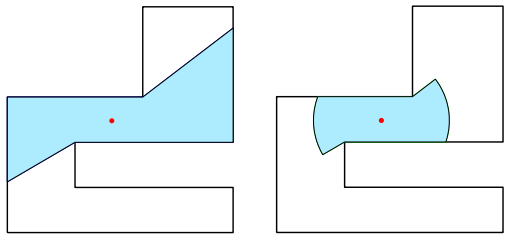

Fig. 1. Graphical representation of the visibility polygon [left] and visibility disc [right] corresponding to red node.

In an area coverage problem mobile robots should plan their motions so that the area sensed is increasing through time. This performance can be represented as the summation of the regions sensed by the nodes and is defined as follows:

$$H = \sum_{i=1}^{n} \int_{W_i} f(x_i; q) \phi(q) \, \mathrm{d}q \ , \tag{4}$$

where $f(x_i; q)$ assesses the performance of the sensor located at x_i in point q, $\phi(q)$ is a density function describing the importance of a point $q \in A$ while W_i is the dominance region assigned to i-th node. The sensing model is assumed to be described by the following performance function:

$$f(x_i, q) = \begin{cases} 1 & \text{if } q \in C_i \\ 0 & \text{otherwise.} \end{cases} \tag{5}$$

One of the most important issues in an area coverage problem is the tessellation of the domain of interest so that the proposed control law is distributed. One common tool for partitioning an area of interest is the Voronoi diagrams that divide the region into subsets, V_i, $i = 1, ..., n$, assigned among the nodes in such a way that each node is responsible for sensing only the points that are closer to it than to any other node.

However, an alternative way of partitioning is needed in the case that the sensing pattern is not a Euclidean disc but a visibility disc, since classical Voronoi diagrams does not take into account nodes' visibility. Therefore the *visibility-based Voronoi diagrams* [23] will be used.

Definition 3: Visibility-based Voronoi diagrams generated by X is the set $V = \left\{V_{vis}^1, ..., V_{vis}^n\right\}$, $i = 1, ..., n$ where V_{vis}^i is called *visibility-based Voronoi cell* of node i and contains the points that are visible to node i and closer to it than to any other node, in case of points visible to other nodes as well:

$$V_{vis}^i = \{q \in VP_i \mid \|q - x_i\| \leq \left\|q - x_j\right\|, \, \forall j \neq i, \, q \in VP_j\} \tag{6}$$

Based on the above definition, neighboring relationships can be determined among the nodes. Thus, two nodes are called visibility-based Delaunay neighbors if they share an edge (or a part of an edge) of their corresponding visibility-based Voronoi cells. The set containing visibility-based Delaunay neighbors of an arbitrary node i, denoted as D_i can be expressed as:

$$D_i = \left\{j \neq i \mid V_{vis}^i \cap V_{vis}^j \neq \varnothing \ \text{(non singleton)}\right\}. \tag{7}$$

Considering the fact that sensors may have a range limited field of view, the *range-limited visibility-based Voronoi diagrams* can be defined.

Definition 4: Range-limited visibility-based Voronoi diagrams generated by X is the set $V_r = \left\{V_{r,vis}^1, ..., V_{r,vis}^n\right\}$, $i = 1, ..., n$ where $V_{r,vis}^i$ is called *range-limited visibility-based Voronoi cell* of node i and contains the points that belong to V_{vis}^i and C_i simultaneously, i.e:

$$V_{r,vis}^i = \{q \in V_{vis}^i \cap C_i\}. \tag{8}$$

Equivalently to the definition of visibility-based power Delaunay neighbors, one can define the range-limited ones. Two nodes are called range-limited visibility based Delaunay neighbors if the intersection of their respective range-limited visibility-based Voronoi cells is non-empty. Thus, the set of the range-limited visibility based Delaunay neighbors of a node i can be written as:

$$D_i^r = \left\{j \neq i \mid V_{r,vis}^i \cap V_{r,vis}^j \neq \varnothing\right\}. \tag{9}$$

Obviously, the Euclidean distance between an arbitrary node i and $j \in D_i^r$ is less than or equal to $2r$ since $\|x_j - x_i\| \leq \|x_c - x_i\| + \|x_c - x_j\| \leq 2r$ where x_c is any point of the set $V_{r,vis}^i \cap V_{r,vis}^j$.

Motivated by this observation, we make the following assumption in order to guarantee that each node can compute its $V_{r,vis}^i$ in a decentralized way:

Assumption 2: Each node can communicate with any other node residing in its communication range defined as:

$$C_i^{com} = \{q \in A | \, \|q - x_i\| \leq 2r\}. \tag{10}$$

Remark 1: Considering definition 3, the following properties for visibility-based Voronoi diagrams are derived:

- Visibility-based Voronoi diagrams cannot provide a full tessellation of the area of interest, which means that $\bigcup_{i=1,...n} V_{vis}^i \subseteq A$. This is a direct consequence of the fact that visibility-based Voronoi diagrams is not a partitioning of the domain A, but a partitioning of the total area visible to the nodes.
- The visibility-based Voronoi cell assigned to an arbitrary node i may be a disconnected or a non–convex set, as depicted in Fig. 2.

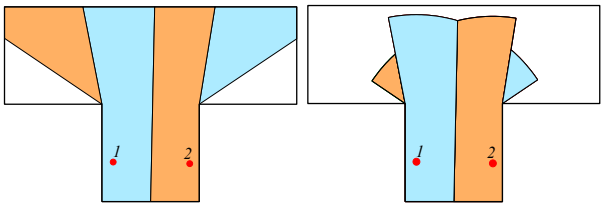

Fig. 2. Graphical representation of the visibility-based Voronoi [left] and range-limited visibility-based Voronoi partitioning [right] generated by two nodes.

Considering the equations (5) and (8) along with the fact that the region covered by the network can be expressed as the union of the corresponding range-limited visibility-based Voronoi diagrams, the area function to be optimized (11) can be written as :

$$H = \sum_{i=1}^{n} \int_{V_{r,vis}^i} \phi(q) \, \mathrm{d}q \ . \tag{11}$$

For simplicity reasons, in the sequel, V_{vis}^i and $V_{r,vis}^i$ are referred to as Voronoi cell and range-limited Voronoi cell of node i respectively.

III. Distributed Control Law

This section is mainly focused on the design of a gradient-based control scheme so that the mobile sensor network optimizes the aforementioned performance function. Before presenting this scheme, let us introduce the notations that will be used in the proof of the proposed control law.

Initially, let us denote the boundary of any set as $\partial(\cdot)$. Thus, the set $\partial(V_{r,vis}^i) \cap \partial(B_i)$ is the set that contains the arcs of B_i that are visible to node i and at the same time belong to $\partial(V_{r,vis}^i)$. Also the set $\partial(VP_i) \bigcap \partial(V_{r,vis}^i)$ contains multiple edges (line segments) belonging both to the visibility polygon of node i, $\partial(VP_i)$, and to $\partial(V_{r,vis}^i)$. Specifically, these edges, may lie either on the boundary of the environment or exclusively on $\partial(VP_i) \bigcap \partial(V_{r,vis}^i)$. The set that contains the latter edges is the $(\partial VP_i \cap \partial V_{r,vis}^i) \setminus \partial A$ and will be denoted as P_i for the sake of simplicity. As depicted in Fig. 3, the set P_i consists of non-intersecting line segments. Introducing the notation $[p_1, p_2]$ for a line segment determined by points p_1 and p_2, the set $(\partial VP_i \cap \partial V_{r,vis}^i) \setminus \partial A$ can be written as:

$$\begin{aligned} P_i &= (\partial VP_i \cap \partial V_{r,vis}^i) \setminus \partial A \\ &= \left\{ \left[p_{a,1}^i, p_{b,1}^i\right] \cup \left[p_{a,2}^i, p_{b,2}^i\right] ... \cup \left[p_{a,k}^i, p_{b,k}^i\right] \right\} \\ &= \bigcup_{l=1,...k} \left[p_{a,l}^i, p_{b,l}^i\right], \end{aligned} \tag{12}$$

where the edges $\left[p_{a,1}^i, p_{b,1}^i\right], \ldots, \left[p_{a,k}^i, p_{b,k}^i\right]$ belong to $\partial(VP_i) \bigcap \partial(V_{r,vis}^i)$ exclusively and $k(i)$ or k for simplicity, is the number of the aforementioned edges, belonging to x_i. Also let $p_{a,l}^i$, $l = 1,...k$ be the point of the segment $\left[p_{a,1}^i, p_{b,1}^i\right]$ which is closest to x_i. In addition to the above, $n_i(q)$ represents the normal, outward unit vector at $q \in \partial V_{r,vis}^i$. Moreover, one can observe that the set $\partial VP_i \setminus \partial A$ contains line segments collinear with a reflex vertex of ∂A. Let denote these reflex vertices as $p_{r,l}^i$. One can easily observe that: $\|x_i - p_{r,l}^i\| \leq \|x_i - p_{a,l}^i\|$.

Fig. 3 illustrates the above notations for two nodes labelled as "1" and "2" respectively. As an example in regard to the node-2, the thick red line represents the arcs of $\partial(V_{r,vis}^2) \cap \partial(B_2)$ while the dark blue segments denote the edges included in P_2. Having introduced these, the main results can be presented.

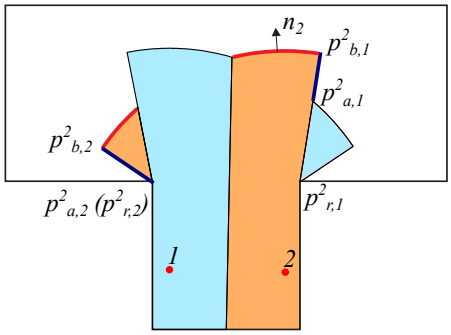

Fig. 3. Graphical representation of notations referred to $V_{r,vis}^2$.

Theorem 1: Considering a group of n mobile nodes equipped with sensors described by (3) being responsible of the sensing coverage of a non-convex domain, the control scheme

$$\begin{aligned} u_i &= \int_{\partial V_{r,vis}^i \cap \partial B_i} \phi(q) n_i(q) \, \mathrm{d}q + \\ &\sum_{l=1,...k} \left\{ -n_i \frac{\left\| p_{b,l}^i - p_{r,l}^i \right\|^2}{\left\| p_{r,l}^i - x_i \right\|} \int_{\delta_{\min}}^{1} \phi(Q) \delta \, \mathrm{d}\delta \right\}, \end{aligned} \tag{13}$$

where $Q = p_{r,l}^i + \delta(p_{b,l}^i - p_{r,l}^i)$ and $\delta_{\min} = \frac{\|p_a - p_r\|}{\|p_b - p_r\|}$, locally

maximizes the area-based criterion (11) in a monotonic manner.

Proof: In order to seek for maximizers of the performance function (11) the first step is to differentiate it with respect to x_i . In this way, we have:

$$\frac{\partial H}{\partial x_i} = \frac{\partial}{\partial x_i}\int_{V^i_{r,vis}} \phi(q)\,\mathrm{d}q + \frac{\partial}{\partial x_i}\sum_{j\neq i}\int_{V^j_{r,vis}} \phi(q)\,\mathrm{d}q \ . \tag{14}$$

Utilizing the Leibniz integral rule [25], equation (14) can be simplified as :

$$\frac{\partial H}{\partial x_i} = \int_{\partial V^i_{r,vis}} \frac{\partial q}{\partial x_i}\phi(q)n_i(q)\,\mathrm{d}q + \sum_{j\neq i}\int_{\partial V^j_{r,vis}} \frac{\partial q}{\partial x_i}\phi(q)n_j(q)\,\mathrm{d}q \ , \tag{15}$$

where $n_i(q)$ is the normal outward unit vector at $q \in \partial V^i_{r,vis}$.

Regarding the first integral, the boundary $\partial V^i_{r,vis}$ can be decomposed on parts that lie either on ∂A, $\partial V^i_{r,vis} \cap \partial V^j_{r,vis}$, $\partial V^i_{r,vis} \cap \partial B_i$, or on P_i. It is worth mentioning to note that the last mentioned set contains edges that belong exclusively on $\partial(VP_i) \bigcap \partial(V^i_{r,vis})$.

Thus, equation (15) can be written as:

$$\begin{aligned}\frac{\partial H}{\partial x_i} \ = \ & \int_{\partial V^i_{r,vis}\cap \partial B_i} \frac{\partial q}{\partial x_i}\phi(q)n_i(q)\,\mathrm{d}q + \int_{P_i} \frac{\partial q}{\partial x_i}\phi(q)n_i(q)\,\mathrm{d}q + \\ & \int_{\partial A \cap \partial V^i_{r,vis}} \frac{\partial q}{\partial x_i}\phi(q)n_i(q)\,\mathrm{d}q + \\ & \sum_{j\neq i}\int_{\partial V^i_{r,vis}\cap \partial V^j_{r,vis}} \frac{\partial q}{\partial x_i}\phi(q)n_i(q)\,\mathrm{d}q + \\ & \sum_{j\neq i}\int_{\partial V^i_{r,vis}\cap \partial V^j_{r,vis}} \frac{\partial q}{\partial x_i}\phi(q)n_j(q)\,\mathrm{d}q \ . \end{aligned} \tag{16}$$

Considering that points $q \in \partial A$ are not affected by infinitesimal maneuvers of node i, it holds that $\frac{\partial q}{\partial x_i} = 0,\ \forall q \in \partial A$ while as far as the points $q \in \partial V^i_{r,vis} \cap \partial V^j_{r,vis}$ are concerned, one can verify that $\frac{\partial q}{\partial x_i} n_i(q) = -\frac{\partial q}{\partial x_i} n_j(q)$.

Consequently, (16) can be simplified as:

$$\frac{\partial H}{\partial x_i} = \int_{\partial V^i_{r,vis}\cap \partial B_i} \frac{\partial q}{\partial x_i}\phi(q)n_i(q)\,\mathrm{d}q + \int_{P_i} \frac{\partial q}{\partial x_i}\phi(q)n_i(q)\,\mathrm{d}q \ . \tag{17}$$

The first integral of (17) can be further simplified considering that all points $q \in \partial V^j_{r,vis} \cap \partial B_i$ move along the direction of node i at the same speed. Hence, it is deduced that in this case:

$$\frac{\partial q}{\partial x_i} = \mathbb{I}, \quad \forall q \in \partial V^i_{r,vis} \cap \partial B_i \ , \tag{18}$$

where $\mathbb{I}$ is the identity matrix.

As for the second integral of (17), the equation that describes the points $q \in P_i$ is needed to be determined. Without loss of generality, let $q \in [p_a, p_b]$ where $[p_a, p_b]$ is an arbitrary edge contained in the set P_i and p_r the reflex vertex corresponding to this edge. Considering these, the demanded equation can be described as:

$$q = p_r + \delta \left\| p_b - p_r \right\| n_c \quad \forall q \in P_i \ , \tag{19}$$

where

- $\frac{\|p_a - p_r\|}{\|p_b - p_r\|} \leq \delta \leq 1$
- n_c is a unit vector defined as $n_c = \frac{p_r - x_i}{\|p_r - x_i\|}$ while it holds that $n_c \perp n_i$.

Taking the partial derivative of (19) w.r.t to x_i we have:

$$\frac{\partial q}{\partial x_i} = \delta \left\| p_b - p_r \right\| \frac{\partial n_c}{\partial x_i} \ , \tag{20}$$

where the Jacobian matrix $\frac{\partial n_c}{\partial x_i}$ is equal to

$$\frac{\partial n_c}{\partial x_i} = \begin{bmatrix} \frac{\partial n_{c,x}}{\partial x_{i,x}} & \frac{\partial n_{c,x}}{\partial x_{i,y}} \\ \frac{\partial n_{c,y}}{\partial x_{i,x}} & \frac{\partial n_{c,y}}{\partial x_{i,y}} \end{bmatrix} = \frac{1}{\left\| p_r - x_i \right\|^3} \begin{bmatrix} a & b \\ c & d \end{bmatrix}, \tag{21}$$

where $a = -\left(p_{r,y} - x_{i,y}\right)^2$, $b = c = \left(p_{r,y} - x_{i,y}\right)\left(p_{r,x} - x_{i,x}\right)$ and $d = -\left(p_{r,x} - x_{i,x}\right)^2$. Note that $p_{r,x}$ and $p_{r,y}$ denote the x and y coordinates of the vector p_r. This notation extends to the vectors n_c, x_i and n_i.

Furthermore, considering that $n_c \perp n_i$, it is concluded that the dot product of these unit vectors equals to zero, i.e:

$$\begin{aligned} n_c \cdot n_i &= \left(p_{r,x} - x_{i,x}, p_{r,y} - x_{i,y}\right) \cdot \left(n_{i,x}, n_{i,y}\right) \\ &= \left(p_{r,x} - x_{i,x}\right) n_{i,x} + \left(p_{r,y} - x_{i,y}\right) n_{i,y} = 0 \ . \end{aligned} \tag{22}$$

Combining equations (21) and (22), the following result is derived:

$$\frac{\partial n_c}{\partial x_i} n_i(q) = \frac{1}{\left\| p_a - x_i \right\|} \begin{bmatrix} -n_{i,x} \\ -n_{i,y} \end{bmatrix} = \frac{1}{\left\| p_r - x_i \right\|}\left(-n_i(q)\right) \ . \tag{23}$$

Following (19) the arc length $\mathrm{d}q$ in the second integral of (17) can be expressed as $\mathrm{d}q = \left\| p_b - p_r \right\| \mathrm{d}\delta$. Also, analyzing the set P_i according to (12) and considering the equations (19), (20) and (23), the second integral of equation (17) can be written as:

$$\sum_{l=1,\ldots k} \left\{ -n_i \frac{\left\| p^i_{b,l} - p^i_{r,l} \right\|^2}{\left\| p^i_{r,l} - x_i \right\|} \int_{\delta_{\min}}^{1} \phi\left(p^i_{r,l} + \delta(p^i_{b,l} - p^i_{r,l}) \right) \delta \,\mathrm{d}\delta \right\} \ . \tag{24}$$

Additionally, the following holds:

$$\frac{\mathrm{d}H}{\mathrm{d}t} = \sum_{i=1,\ldots,n} \frac{\partial H}{\partial x_i}\frac{\mathrm{d}x_i}{\mathrm{d}t} = \sum_{i=1,\ldots,n} \left\| u_i \right\|^2 \geq 0 \ , \tag{25}$$

proving that the proposed control law (13) leads to gradient flow along nodes' trajectories, which completes the proof. ■

The control law (13) is explained in Fig. 4, where a single node has been placed is a simple Γ-shaped environment. The control input of the node has been analyzed into two components. The first one (orange) stands for the first term of (13), which is defined over the arcs $\partial V^i_{r,vis} \cap \partial B_i$, while the second one (blue) represents the second term in (13). The direction of the blue vector denotes the optimal increase of the node's visibility polygon VP_1. The resulting control action corresponds to the black vector.

Remark 2: The proposed control law is characterized by a distributed nature since for the evaluation of visibility-based Voronoi diagrams and of sets P_i only the range-limited visibility-based Delaunay neighbors' coordinates are needed.

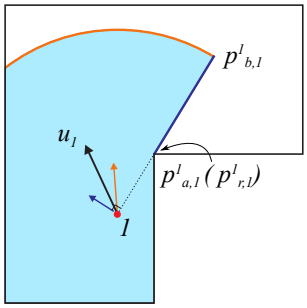

Fig. 4. Graphical representation of the proposed control law.

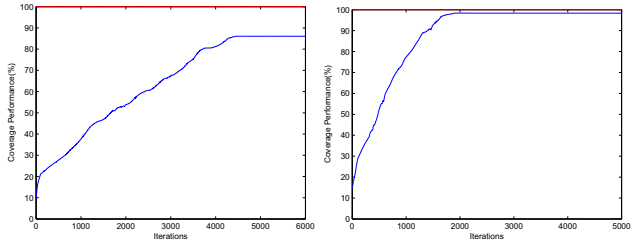

Fig. 7. Coverage performance (blue line) w.r.t iterations for the first [left] and the second [right] simulation study.

Remark 3: In case the control law (13) leads a node in a position outside of the domain of interest, that node should move along a suboptimal direction determined by the projection of the gradient direction to the boundary of the environment.

Remark 4: If the set P_i is empty (such as on a convex area for surveillance) then the control law (13) is degenerated into that proposed in [5].

IV. Simulation Studies

In this section, simulation studies are presented in order to verify the results obtained in the previous section. It should be noted that throughout these simulations the density function has been set to unity for all the points in the environment, i.e. $\phi(q) = 1,\ \forall q \in A$.

In the first simulation, the considered concave domain is surveyed by a group of $n = 15$ nodes equipped with sensors of sensing radius $r = 0.6$ units. The initial network configuration is depicted in the left part Fig. 5 while the nodes' trajectories through time and the final network configuration are presented in the middle and the right part of the same figure, respectively. Nodes are initially deployed in the left down corner of the domain and in the final state nodes have reached a local maximum of performance function (11), sensing 86% of the whole area (Fig. 7) which is quite satisfactory considering the complexity of the environment. Also the trajectories of the nodes indicate that they tend to follow in groups roughly the same path while traversing part of the environment.

Another simulation study is provided in Fig. 6 where $n = 13$ robots with sensing range $r = 0.6$ units should sense a non-convex domain of total area 9.5 units^2. Nodes are initially positioned as depicted in the upper left part of Fig. 6 sensing 14.7% of the whole domain while according to their sensing capabilities a full area coverage can be achieved. Applying the proposed control scheme to the network, nodes evolved as presented in the middle part of the aforementioned figure until they reach the final state depicted in the right part of the same figure. Coverage performance is visualized in the right part of Fig. 7 and one can observe that increases at each iteration until it converges to 98.3%, which is very close to the maximum possible performance. This simulation study is presented in the video accompanying this paper.

V. Conclusions

A distributed visibility-based coordination scheme was presented for the coverage problem of non-convex domains that monotonically maximizes the area covered by the network, considering that nodes are equipped with range-limited visibility-based sensors such as omnidirectional cameras. The proposed control law was based on a mixture of classical Voronoi tessellation and on nodes' visibility extending a class of algorithms used in coverage of convex environments. Simulation studies were carried out verifying the effectiveness of the proposed control scheme.

References

[1] S. Li, A. Zhan, X. Wu, and G. Chen, "ERN: emergence rescue navigation with wireless sensor networks," in *Parallel and Distributed Systems (ICPADS), 2009 15th International Conference on*. IEEE, 2009, pp. 361–368.

[2] K. Alexis, G. Nikolakopoulos, A. Tzes, and L. Dritsas, *Applications of Intelligent Control to Engineering Systems*, ser. Intelligent Systems, Control and Automation: Science and Engineering. Springer Science, 2009, vol. 39, ch. 7: Coordination of Helicopter UAVs for Aerial Forest–Fire Surveillance, pp. 169–193.

[3] Y. Koveos, A. Panousopoulou, E. Kolyvas, V. Reppa, K. Koutroumpas, A. Tsoukalas, and A. Tzes, "An integrated power aware system for robotic-based lunar exploration," in *Proc. IEEE/RSJ International Conference on Intelligent Robots and Systems IROS 2007*, San Diego, CA, USA, 2007, pp. 827–832.

[4] J. Cortés, S. Martinez, T. Karatas, and F. Bullo, "Coverage control for mobile sensing networks," *IEEE Transactions on Robotics and Automation*, vol. 20, no. 2, pp. 243–255, 2004.

[5] J. Cortés, S. Martinez, and F. Bullo, "Spatially-distributed coverage optimization and control with limited-range interactions," *ESAIM: Control, Optimisation and Calculus of Variations*, vol. 11, no. 4, pp. 691–719, 2005.

[6] L. Lazos and R. Poovendran, "Stochastic coverage in heterogeneous sensor networks," *ACM Transactions on Sensor Networks*, vol. 2, no. 3, pp. 325–358, 2006.

[7] N. Bartolini, T. Calamoneri, T. La Porta, and S. Silvestri, "Autonomous deployment of heterogeneous mobile sensors," *IEEE Transactions on Mobile Computing*, vol. 10, no. 6, pp. 753–766, 2011.

[8] Y. Stergiopoulos and A. Tzes, "Convex Voronoi-inspired space partitioning for heterogeneous networks: A coverage-oriented approach," *IET Control Theory and Applications*, vol. 4, no. 12, pp. 2802–2812, 2010.

[9] A. Gusrialdi, T. Hatanaka, and M. Fujita, "Coverage control for mobile networks with limited-range anisotropic sensors," in *Decision and Control, 2008. CDC 2008. 47th IEEE Conference on*. IEEE, 2008, pp. 4263–4268.

[10] K. Laventall and J. Cortés, "Coverage control by robotic networks with limited-range anisotropic sensory," in *Proc. of the 2008 American Control Conference*, Seattle, Washington, USA, 2008, pp. 2666–2671.

[11] Y. Stergiopoulos and A. Tzes, "Spatially distributed area coverage optimisation in mobile robotic networks with arbitrary convex anisotropic patterns," *Automatica*, vol. 49, no. 1, pp. 232–237, 2013.

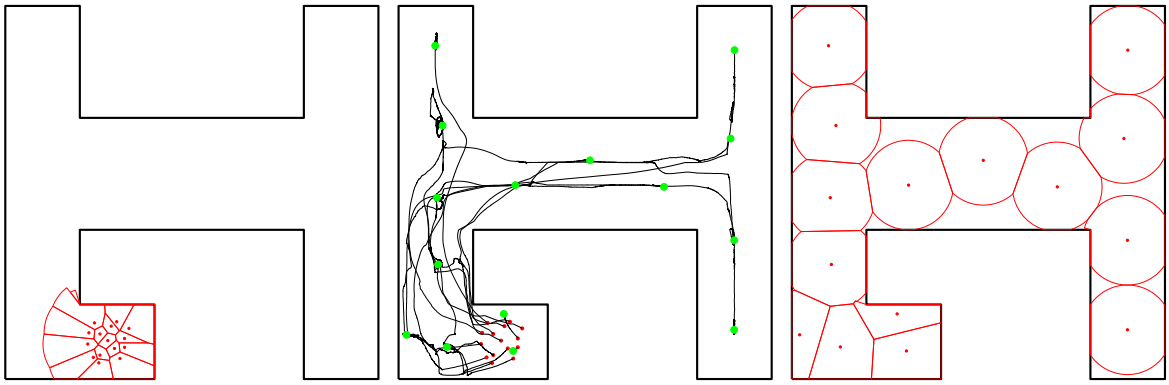

Fig. 5. Simulation study I: [Left] Initial network configuration. [Middle] Network evolution. The green (red) dots represent the nodes' final (initial) positions. [Right] Final network state.

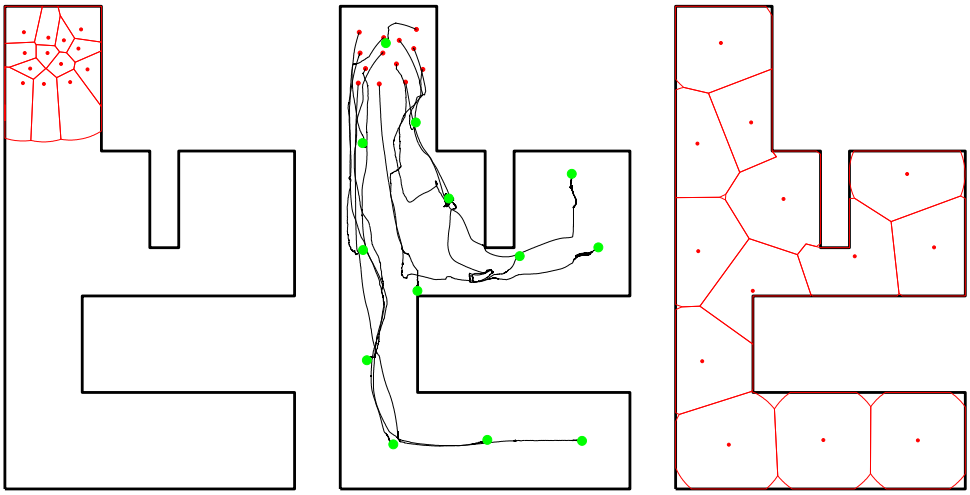

Fig. 6. Simulation study II:[Left] Initial network configuration. [Middle] Network evolution. The green (red) dots represent the nodes' final (initial) positions. [Right] Final network state.

[12] Y. Stergiopoulos, Y. Kantaros, and A. Tzes, "Connectivity-aware coordination of robotic networks for area coverage optimization," in *Industrial Technology (ICIT), 2012 IEEE International Conference on*. IEEE, 2012, pp. 31–35.

[13] ——, "Distributed Control of Mobile Sensor Networks under RF Connectivity Constraints," *International Journal of Distributed Sensor Networks*, vol. 2012, 2012.

[14] C. Caicedo-Nunez and M. Zefran, "Performing coverage on non-convex domains," in *IEEE International Conference in Control Applications*, San Antonio, Texas , USA, 2008, pp. 1019–1024.

[15] C. Caicedo-Nuez and M. Zefran, "A coverage algorithm for a class of non-convex regions," in *Decision and Control, 2008. CDC 2008. 47th IEEE Conference on*. IEEE, 2008, pp. 4244–4249.

[16] L. Pimenta, V. Kumar, R. C. Mesquita, and G. Pereira, "Sensing and coverage for a network of heterogeneous robots," in *Decision and Control, 2008. CDC 2008. 47th IEEE Conference on*. IEEE, 2008, pp. 3947–3952.

[17] S. Bhattacharya, N. Michael, and V. Kumar, "Distributed coverage and exploration in unknown non-convex environments," *Distributed Autonomous Robotic Systems*, pp. 61–75, 2010.

[18] A. Breitenmoser, M. Schwager, J.-C. Metzger, R. Siegwart, and D. Rus, "Voronoi coverage of non-convex environments with a group of networked robots," in *Robotics and Automation (ICRA), 2010 IEEE International Conference on*. IEEE, 2010, pp. 4982–4989.

[19] A. Howard, M. J. Mataric, and G. S. Sukhatme, "Mobile sensor network deployment using potential fields: A distributed, scalable solution to the area coverage problem," in *Proceedings of the 6th International Symposium on Distributed Autonomous Robotics Systems (DARS02)*. Citeseer, 2002, pp. 299–308.

[20] A. Renzaglia, A. Martinelli, *et al.*, "Distributed coverage control for a multi-robot team in a non-convex environment," in *IEEE IROS09 3rd Workshop on Planning, Perception and Navigation for Intelligent Vehicles*, 2009.

[21] M. Thanou, Y. Stergiopoulos, and A. Tzes, "Distributed coverage using geodesic metric for nonconvex environments," in *Robotics and Automation (ICRA), 2013 IEEE International Conference on*, Karlsruhe, Germany, May 2013, pp. 925–930.

[22] ——, "Distributed coverage of mobile heterogeneous networks in non–convex environments," in 21st *Mediterranean Conference on Control and Automation*, Platanias-Chania, Crete, Greece, June 2013, pp. 956–962.

[23] L. Lu, Y.-K. Choi, and W. Wang, "Visibility-based coverage of mobile sensors in non-convex domains," in *Voronoi Diagrams in Science and Engineering (ISVD), 2011 Eighth International Symposium on*. IEEE, 2011, pp. 105–111.

[24] A. Ganguli, J. Cortés, and F. Bullo, "Distributed coverage of nonconvex environments," in *Networked Sensing Information and Control (Proceedings of the NSF Workshop on Future Directions in Systems Research for Networked Sensing*, 2006, pp. 289–305.

[25] H. Flanders, "Differentiation under the integral sign," *American Mathematical Monthly*, vol. 80, no. 6, pp. 615–627, 1973.